IEEE Open Journal of
Intelligent Transportation
Systems

Received 30 October 2022; revised 15 March 2023; accepted 21 May 2023. Date of publication 2 June 2023; date of current version 23 June 2023.

Digital Object Identifier 10.1109/OJITS.2023.3282237

HISS: A Pedestrian Trajectory Planning Framework Using Receding Horizon Optimization

SAUMYA GUPTA[1], MOHAMED H. ZAKI[2] (Member, IEEE), AND ADAN VELA[3]

[1]Civil, Environmental, and Construction Engineering Department, University of Central Florida, Orlando, FL 32816, USA

[2]Department of Civil and Environmental Engineering, Western University, London, ON N6A 3K7, Canada

[3]Industrial Engineering and Management Systems Department, University of Central Florida, Orlando, FL 32816, USA

CORRESPONDING AUTHOR: S. GUPTA (e-mail: saumya.gupta@knights.ucf.edu)

This work was supported in part by the UCF College of Graduate Studies Open Access Publishing Fund.

ABSTRACT The paper proposes a generative pedestrian trajectory modeling framework named HISS - Human Interactions in Shared Space. The trajectory modeling framework is based on a receding horizon optimization approach utilizing pedestrian behavior and interactions that seeks to capture pedestrian trajectory planning and execution. The benefit of the proposed dynamic optimization trajectory generation approach is that it requires minimal calibration data under a variety of traffic scenarios. In this paper, we formalize several pedestrian-pedestrian interaction scenarios and implement trajectories' conflict avoidance through mixed integer linear programming (MILP). We validate the proposed framework on two benchmark datasets - DUT and TrajNet++. The paper shows that when the framework's parameters are tuned to certain initial conditions and pedestrian behavior and interaction rules, the framework generates pedestrian trajectories similar to those observable in real-world scenarios, justifying the framework's capability to provide explanations and solutions to various traffic situations. This feature makes the proposed framework useful for modelers and urban city planners in making policy decisions.

INDEX TERMS Pedestrian behavior, active mobility, trajectory planning, trajectory generation, receding horizon control, mixed integer linear programming.

I. INTRODUCTION

ONE RECENT trend in urban planning is to promote walking, cycling, and other contemporary modes of micro-mobility (e.g., e-bicycles, e-scooters) as viable commute options in cities. These commute choices benefit from coordinated city planning and infrastructure design to support and ease their daily and regular utilization. One city design approach called *shared spaces* is gaining attention as a potential solution to urban transportation challenges of traffic movement, congestion, and pedestrian safety. Shared space is an urban planning design approach where humans and vehicles share a common physical space without the traditional safety measures of traffic lights, curbs, and traffic rules [1]. The premise behind shared spaces is to promote road users' safety and accessibility through the reconceptualization and redesign of roadways. Concurrent with spaced spaces, urban city planners are aiming to incorporate intelligent transportation systems into a city's infrastructure to enable smart mobility to improve safety, alleviate congestion, and promote active mobility.

For modern approaches like shared spaces, intelligent transportation systems, and smart cities humans are at the core of any traffic design process, and yet, recent reports indicate that there has been a 53% upsurge in pedestrian fatalities during the previous ten years [2], [3]. This contrast in pedestrian impacts highlight the critical need to identify pedestrian safety challenges in traditional and modern city planning, in particular, understanding and characterizing pedestrian behaviors when interacting with and amongst diverse traffic. To actualize shared spaces, the focus should expand consideration to safety of pedestrians and other micro-mobility users.

One manner in which to aid in the design of shared spaces is through the application of modeling and simulation. Through focused consideration of pedestrian behaviors and

The review of this article was arranged by Associate Editor Winnie Daamen.

interactions within a modeling and simulation framework researchers can aid in ensuring (a) smooth and safe navigation of nominal traffic, (b) better crowd management during social events, and (c) improved traffic infrastructure design applicability and reliability. Moreover, within a simulation framework, we can explore a range of scenarios to better understand pedestrian interactions with each other, as well as pedestrian interactions with other micro-mobility agents. These complex **pedestrian interaction scenarios** and their responses to such interactions make pedestrian trajectory modeling and simulation challenging.

In recent decades significant research has been focused on developing accurate and easy-to-tune pedestrian trajectory modeling and simulation tools. Towards this goal, substantial effort has been put into understanding and modeling pedestrian behaviors [4], and movements [5]. Broadly speaking, pedestrians exhibit distinct dynamics and interaction behaviors depending on the environment and underlying scenario, e.g., individual vs. group travel, and dense vs. sparse walking environments. Therefore, an efficient and realistic pedestrian trajectory modeling requires (a) consideration of pedestrian behavioral and interaction rules and (b) inclusion of environmental features.

Scope: This paper aims to develop a pedestrian trajectory modeling framework that is (a) generative, (b) representative of pedestrian behavior and interaction rules, (c) broadly transferable across different traffic scenarios and locations, and (d) requires minimal data to calibrate the model parameters. We propose a generative pedestrian trajectory modeling framework based on a receding horizon optimization approach utilizing pedestrian behavior and interactions that realistically captures pedestrian trajectory planning and execution. Our previous work [6] has addressed the pedestrian interactions involving the dynamics of a group of pedestrians walking together, and the dynamics of groups of pedestrians and their interactions with stationary obstacles. Here we extend on our previous work by formalizing pedestrian behaviors and interactions of groups of pedestrians avoiding conflicts with other pedestrians traversing in the same space.

Approach Overview: The proposed framework is based on the concept of optimization embedded within feedback control. The trajectory generation problem is formulated as a mixed integer linear program (MILP) within the receding horizon framework. MILP aids in the efficient solution of the non-convex formulation induced by the inclusion of obstacle avoidance and conflict avoidance constraints [7], [8].

In this paper, we assume pedestrians plan their trajectories looking forward over a time window, based on their line of sight and immediate environmental factors. As pedestrians move along their planned trajectory they continue to reassess their plans, making adjustments as needed in response to obstacles and other moving agents in the area. Thus a dynamic optimization approach is appropriate to capture the pedestrian planning and execution process. We represent the ongoing optimization dynamic by utilizing receding horizon control (RHC) into the modeling framework. The incorporation of RHC enables a mechanism to incorporate feedback after fixed, regular intervals during trajectory planning. As such, the pedestrian trajectory planning and execution model generates trajectories by solving optimization problems over a sequence of short time-horizons, with most recent states are used as initial states at each iteration.

The proposed framework is tested for pedestrian interactive case scenarios such as moving obstacle (conflict) avoidance. The framework is assessed using two benchmark datasets, (a) the Dalian University of Technology (DUT) and (b) the TrajNet++ dataset. Case studies demonstrated that generated trajectories uphold near-zero Mean Euclidean Distance and Final Displacement Error with real trajectories, thereby validating the model.

Contributions and Key Features: This paper focuses on formalizing several pedestrian-pedestrian interaction scenarios related to conflict avoidance which is critical for the completeness of a trajectory generation framework. The work presented here extends our previous work by augmenting the framework's capabilities to include conflict avoidance between pedestrians and groups of pedestrians while generating realistic conflict-free pedestrian trajectories. The conflict avoidance problem is formulated utilizing a MILP approach.

The specific features of the proposed approach are as follows:

- The framework is built using optimization, which aligns well with our conceptualization of how pedestrians plan trajectories in the presence of moving obstacles.
- The trajectory planning problem is cast as a MILP to address the complexities of non-convex optimization introduced by conflict avoidance constraints.
- The incorporation of Receding Horizon Control makes use of ongoing optimization that mimics a pedestrian's dynamic trajectory planning and implementation.
- The framework is capable of handling both stationary obstacles and conflict avoidance with moving objects.
- The framework utilizes relatively a few parameters that can be computed with limited data availability.

The proposed framework is capable of successfully generating dynamically feasible and naturalistic pedestrian trajectories under a range of scenarios. The framework is robust and generalizable - meaning that the calibrated parameters can be transferred to similar behavioral scenarios at other traffic locations. The specific features of the proposed framework, together with the generalizability of the framework - meaning that the calibrated parameters can be transferred to similar behavioral scenarios at other traffic locations, make the framework unique.

II. LITERATURE REVIEW: PEDESTRIAN MODELING APPROACHES

The decision-making of a pedestrian is affected by several factors such as physical, mental, psychological, and environmental conditions. It is well established in the literature that having the freedom to execute their movements,

pedestrians exhibit the least predictable behavior and do not always follow an expected logical pattern. Therefore, it is not trivial to model pedestrian trajectories [9]. The last two decades of the twentieth century have witnessed significant efforts towards pedestrian motion analysis through pedestrian detection, tracking, and understanding its behavior [10], [11]. The computer vision and pattern recognition techniques, showed substantial progress in the automatic capture of human movement and its analysis, thereby helping in understanding pedestrian behavior [12].

Pedestrian modeling approaches are wide-ranging, including macroscopic pedestrian flow analysis, evacuation strategies during disasters, and crowd behavior to individual-level behavior modeling. The early research described the pedestrian movement using a) physical models based on *social force* and *Newtonian mechanics*, and b) models based on the *Cellular Automata* (CA) paradigm. Physical models describe the pedestrian movement as the sum of attractive and repulsive force vectors [13]. Whereas, in CA-based models, the street and environment are represented as matrices of cells; a pedestrian can only move from cell to cell in a given model iteration depending on pre-defined transition rules dictating the next moves. The CA-based pedestrian modeling approach was explored by Blue and Adler [14]. The study in [15] provides an extensive comparison of existing micro and macro pedestrian motion models (e.g., social force-based, cellular automata based, velocity-based models, hybrid models, and behavioral models). It concludes that none of the assessed models is capable of simulating pedestrian/crowd behavior realistically.

With the increase in computing power, a shift has been seen from aggregate to individual level (microscopic) modeling. It has become more practical in recent times, and the progression is seen since the development of automata approaches [16], [17]. Agent based modeling (ABM) approaches provide a new paradigm for pedestrian simulation. It enables a realistic simulation of pedestrian behavior by considering agents (pedestrians) as rational entities that a) are autonomous (can decide their motion independently), b) are heterogeneous (not all pedestrians are assumed to behave in the same fashion), c) learn from their environment, and d) adapt their behavior according to environmental changes [18]. The ABM models were found to be suitable for modeling complex pedestrian behavior and capturing complex real-world pedestrian-pedestrian and pedestrian-traffic interaction scenarios [19], [20], [21]. However, there are certain limitations to the ABM approach. Since the approach is based on microscopic individual agent modeling dependent upon initial conditions, the results are not reproducible enough. I.e., changes in initial conditions lead to different simulation outputs. Moreover, the individual-level details are difficult to quantify and calibrate, often requiring a large number of parameters to be tuned, limiting the range of agent representation and, consequently, the model's utility in the understanding of the real world [22]. There is also the use of inverse reinforcement learning to predict pedestrian behavior and interactions [23]. Nonetheless, every model has its own characteristics, advantages, and disadvantages; making them suitable for different applications. For further discussion on the current state-of-the-art pedestrian modeling approaches, readers are referred to our previous related article [6].

Previous Work and Knowledge Gaps: In our previous related work [6], we developed a pedestrian trajectory modeling approach incorporating pedestrian behavior and interaction rules. The model was generative, could represent a range of interaction scenarios, and required minimal data to calibrate the model parameters. The model was validated for scenarios involving two and three pedestrians walking in a group and their interactions with a stationary obstacle (e.g., a tree). However, a significant shortcoming in the previous work was that it lacked the ability to maneuver in the presence of moving objects (e.g., other pedestrians, micro-mobility agents). In other words, the previous work lacked the conflict avoidance capabilities of a pedestrian (or group of pedestrians). This severely limited the applicability of the model to simulate realistic scenarios. Conflict avoidance is crucial for realistic pedestrian modeling. However, including pedestrian behavior and interaction rules involving moving obstacles (such as another pedestrian) is not trivial. The pedestrian has unpredictable, complex walking behavior; the interactions with a moving obstacle are complicated and involve multiple behavioral factors.

III. PEDESTRIAN BEHAVIOR AND INTERACTIONS IN SHARED SPACE

The proposed research is based on observations of the pedestrians' movement and the literature on pedestrian traffic behavior and interaction rules [24], [25], [26], [27], [28], [29], [30], [31]. For instance, the movement of an individual pedestrian depends on how the pedestrian observes the surroundings and processes the observed information, e.g., intuitively estimating the distance of the obstacle to adapt their walking. Additionally, when expanded to a group of pedestrians, the pedestrian interactions with the surroundings and their interactions within the group have to be understood. Next, we briefly describe these interactions.

Trajectory Categorization: Pedestrian motion is *characterized* by their behavior and social interactions such as human-human and human-environment interactions. Based on the observation of pedestrian trajectories in TrajNet++ data, [32] classifies them into three broad categories - linear, static, and non-linear. To classify each of these broad trajectory categories effectively a pedestrian of interest, *primary pedestrian*, is chosen in a traffic scene. Each of these trajectories is described below:

A *linear trajectory* occurs when the primary pedestrian (having no interactions) maintains an almost linear movement in the direction of motion. A *static trajectory* where the primary pedestrian exhibits limited movement, eg. the case where the pedestrian is standing and talking with another person. The *non-linear trajectory* is the category

with 'non-linear' pedestrian trajectories (with or without interactions). The non-linear (interacting) trajectory is the most challenging to model and is of interest to us in this paper. The trajectories are referred to as *interacting* when the primary pedestrian undergoes social (i.e., human-human) interactions. The non-linear interaction trajectory categories can be further classified as follows:

- *Group Interaction trajectory:* When the primary pedestrian maintains a group by keeping a close and comfortable distance with their neighbor [26], [29].
- *Conflict Avoidance trajectory:* When a primary pedestrian avoids a collision with another pedestrian or a group of pedestrians crossing paths. The conflict avoidance can be further classified as line-of-sight conflict avoidance (see Figures 1(a) and 1(b)) or in the field-of-view conflict avoidance (see Figures 2(a), 2(b)). The conflict avoidance category also includes trajectories of social interactions where a primary pedestrian follows another walking pedestrian while maintaining a safe following distance.
- *Other Interactions trajectory:* This category includes the trajectories where the primary pedestrian interacts with various active mobility traffic agents such as a cyclist and e-bikes.

The defined pedestrian trajectory categorization is useful in trajectory modeling as it helps to identify the case studies and scenarios critical for successful modeling.

IV. SCENARIO SELECTION AND PARAMETER DESIGN

In this paper, the pedestrian trajectory planning framework accounts for traffic interaction scenarios involving conflict avoidance with other moving pedestrians or a group of pedestrians moving in the pedestrian's *line-of-sight*, or the *field-of-view*. Accounting for pedestrian social interactions with other moving obstacles is critical for pedestrians' trajectory planning. This works augment our previous research work in we analyzed the traffic scenarios of group interactions between two and three pedestrians, and pedestrians avoiding a stationary obstacle. The moving objects seen or not seen during trajectory planning depend on pedestrian's visual acuity, central vision field, peripheral vision field, surrounding activities, and many other traffic distractions [33], [34]. This necessitates updating the planned pedestrian's trajectory at regular short intervals.

In this paper, we will focus on the following pedestrians' conflict avoidance traffic scenarios that are critical for trajectory generation modeling.

- *Line-of-sight Conflict Avoidance (LCA):* An individual pedestrian (or a group) avoids another moving pedestrian (or a group) coming from the opposite direction. See Figure 1(a) and Figure 1(b). The line-of-sight (LoS) means that an agent has an unobstructed view along the straight line of an object.
- *Field-of-view Conflict Avoidance (FCA):* A moving pedestrian (or group of pedestrians) lies in the field-of-view (FoV) of the primary pedestrian (or group of pedestrians). See Figure 2(a) and Figure 2(b).

A. DESIGNED BEHAVIORAL PARAMETERS

The pedestrian interactions with a moving obstacle are complicated and involve multiple behavioral factors. Modeling conflict avoidance traffic scenarios is crucial for developing a pedestrian trajectory generation framework, also, it is not a trivial task. This necessitates defining new pedestrian's behavioral parameters. We introduce the behavioral parameters by building on the chosen conflict avoidance traffic scenarios in the previous Section IV. These parameters are indicative of characteristic behavior during conflict avoidance. The description of proposed parameters is described below and summarized in Table 1.

***LCA* - Individual and Group Scenarios:** In Figure 1(a) (and 1(b)), we observe two pedestrians (or groups) moving straight towards each other; they are in each other's line-of-sight (LoS). The LoS means that an agent has an unobstructed view along the straight line of an object. In such cases, intuitively, pedestrians' change the direction of motion slightly so that they can avoid a collision. In the figures, d_1^{ILS} (or d_1^{GLS}) represents the distance between the collision point and pedestrian (or group) when the direction of motion starts to change. The d_2^{ILS} (or d_2^{GLS}) distance is the minimum safe distance between two pedestrians (or groups) when they pass each other. In this scenario, both pedestrians (or groups) are responsible for maintaining a safe distance as both can see each other. Note that the exact alteration in their trajectories might differ (one might change their trajectory more than the other). However, for the modeling purpose, we only require d_2^{ILS} and d_2^{GLS}. Note that both d_1^{IFV} and d_2^{IFV} would be greater (or equal to) than the minimum comfortable distance between two pedestrians. Their actual values will depend from case to case; however, an average of the values observed in a dataset would suffice in the algorithm.

***FCA* - Individual and Group Scenarios:** In Figure 2(a) (and 2(b)), we consider the case(s) where a pedestrian (or group) lies in another pedestrian's (or group's) field-of-view (FoV). In such scenarios, only the pedestrian (or group) who can see the other pedestrian (or group) present in its FoV re-plans its trajectory to avoid the collision. In Figure 2(a), a pedestrian B (with a stroller) is moving in the FoV of another pedestrian A. If pedestrian A does not change the trajectory (motion direction or speed), then there are high chances of them getting too close to be comfortable or even colliding. The *red* and *green crosses* indicate their corresponding positions in the pre-collision (unaltered) approach. Pedestrian A starts altering its trajectory at a distance d_1^{IFV} (the distance between red and green crosses). The altered trajectory of pedestrian A crosses the trajectory of pedestrian B at the *green dot*; in the meantime, pedestrian B has moved to the red dot on its unaltered trajectory. The *red* and *green dots* indicate their corresponding positions in the post-collision (altered) approach. d_2^{IFV} is the distance between the

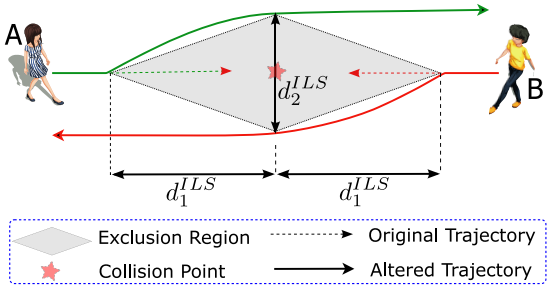

(a) Line-of-sight conflict avoidance between two pedestrians

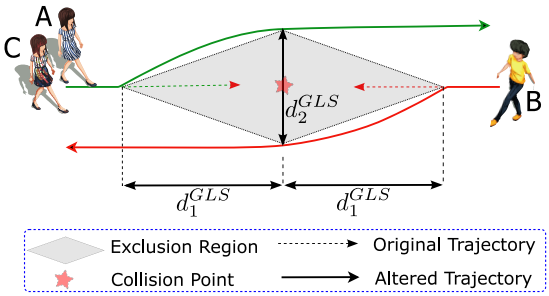

(b) Line-of-sight conflict avoidance between a pedestrian and a group of pedestrians

FIGURE 1. **Line-of-sight Traffic Scenarios and Designed Behavioral Parameters.**

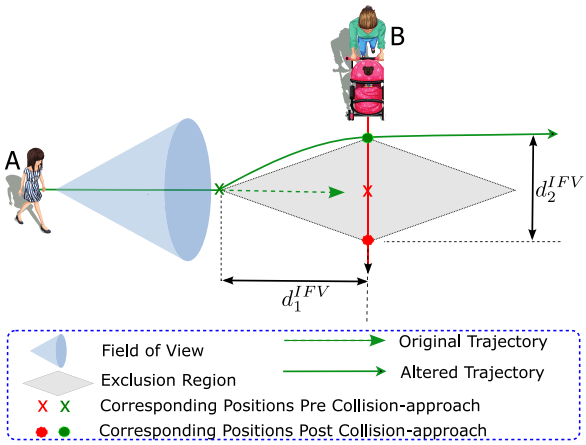

(a) Field-of-view conflict avoidance between two pedestrians

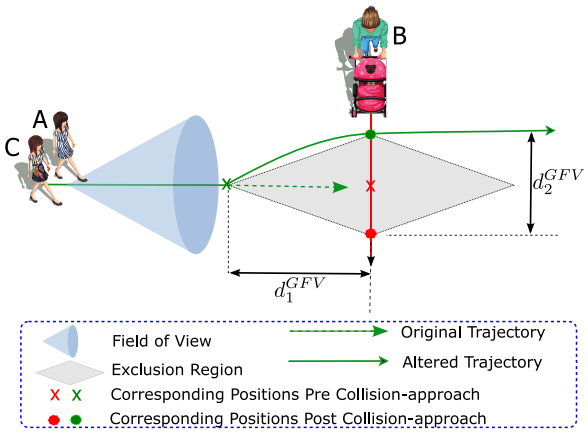

(b) Field-of-view conflict interaction between a pedestrian and a group of pedestrians

FIGURE 2. **Field-of-view Traffic Scenarios and Designed Behavioral Parameters.**

TABLE 1. **Description of proposed parameters.**

Parameter	Description
d_1^{ILS} (& d_1^{GLS})	Euclidean distance between the collision point and the point at which two pedestrians (or groups) start to change their trajectory to avoid the collision and keep a comfortable distance between them.
d_2^{ILS} (& d_2^{GLS})	Euclidean distance between two points at which two pedestrians (or groups) directly moving towards each other come closest and pass each other while maintaining a minimum safe distance required to avoid a collision. In many cases, this Euclidean distance segment will be perpendicular to the direction of their motion. In other words, d_2^{ILS} is the length of the line segment between the two closest points on the individual pedestrian's trajectories. Note that we measure the distance from the trajectory representing their center of mass for the pedestrian group.
d_1^{IFV} (& d_1^{GFV})	Euclidean distance between the pedestrians when the primary pedestrian (or group) (with another pedestrian in its FOV) starts to change its trajectory to avoid the collision and keep a comfortable distance between them.
d_2^{IFV} (& d_2^{GFV})	Euclidean distance between the pedestrians (or groups) when they come closest and pass each other while maintaining a minimum safe distance required to avoid a collision. In other words, d_2^{IFV} is the length of the line segment between the two closest points on the individual pedestrian's trajectories on the post-collision approach. Note that for the group of pedestrians, we measure the distance from the trajectory representing their center of mass.

two pedestrians when their trajectories intersect. Note that both d_1^{IFV} and d_2^{IFV} would be greater than the minimum comfortable distance between two pedestrians. Their actual value will depend from case to case; however, an average of the values observed in a dataset would suffice for the algorithm.

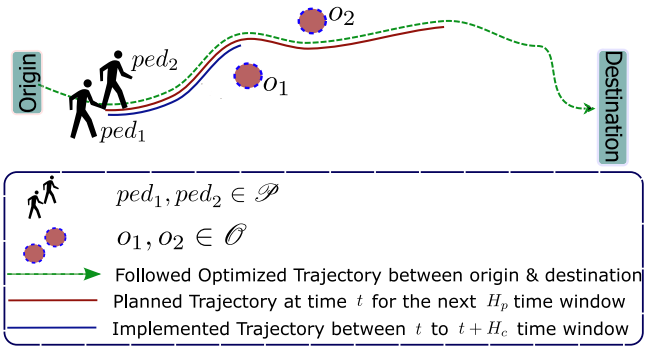

FIGURE 3. Planning and Control Window Trajectories.

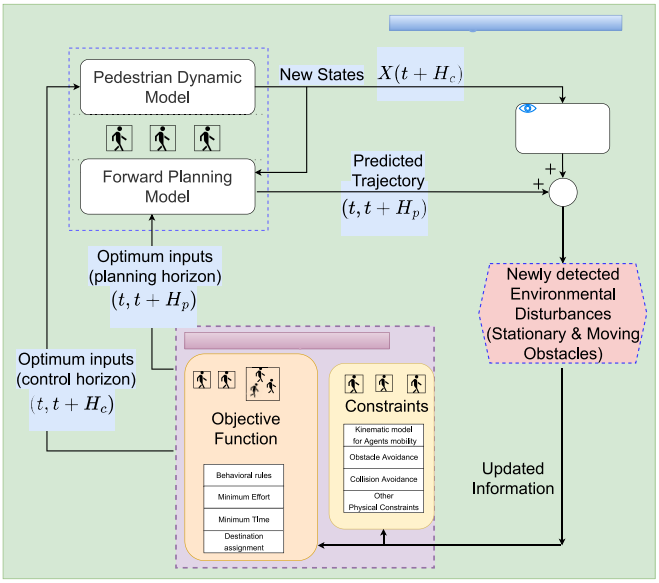

FIGURE 4. HISS framework: MILP based optimization embedded in the Receding Horizon Control Loop.

V. PROPOSED MODELING FRAMEWORK

In this section, firstly, we briefly describe the trajectory planning problem and then specify our research approach to the pedestrian trajectory planning problem. *Trajectory planning problem* are often solved using optimization to generate a collision-free path over time from an initial to a final point in a specified environment. These optimization algorithms generate trajectories when considering a variety of optimality criteria such as minimum time, minimum energy, minimum jerk, or a weighted combination of them. The key ingredients of these algorithms include the designed optimality criteria (objective function), description of state and decision variables, kinematics dynamics of the considered agent, and constraints of the obstacles in the environment. Output is a trajectory expressed as a sequence of values of position, velocity, and acceleration at regular time intervals [35], [36]. Optimization-based trajectory planning has been used extensively for robots, UAVs, and aircraft [37].

Research Approach: Section IV-A discussed the pedestrians' interaction complexities and behavioral parameters, which play an integral role in the development of the framework [38], [39]. We propose a control-based pedestrian trajectory generation framework with multi-criteria optimization that considers minimum energy and pedestrian social interaction rules. The HISS (Human Interaction in Shared space) framework is formulated as a MILP embedded within RHC. The design of RHC embedding, objective function, and constraints are discussed below.

When traversing an environment, we assume pedestrians will become aware of changes in their surroundings (e.g., the arrival of impediments). Consider Figure 3 for one such example. While planning their trajectory to the terminus, pedestrians ped_i and ped_j will advance via a series of segments characterized by an ordered set of way-points before arriving at their destination. Figure 4 illustrates a receding horizon control framework that initiates with every pedestrian maintaining an awareness of their subsequent chosen way-point, the other pedestrians they are walking with (if any), and the local surroundings (i.e., the obstructions and other pedestrians not in their group). Considering these factors, a pedestrian is modeled to plan path H_p seconds into the future (referred to as the planning horizon). Now, based on the receding horizon approach, a pedestrian executes their planned path for a fixed H_c seconds (referred to as the control horizon), where $H_c << H_p$. After the executed path of H_c seconds, the planning process looking H_p seconds is repeated. This path planning and path execution process happens ad infinitum until the pedestrian reaches the way-point and ultimately their final destination. At each iteration, the pedestrian revises their estimate of the surroundings, and the position of other pedestrians and obstacles. As the pedestrian arrives at their desired way-point, a new way-point is established, and the procedure repeats. Note that the proposed trajectory planning process can be easily adapted to the trajectory planning of other active mobility agents.

Within the RHC loop, a MILP optimization is introduced which incorporates pedestrian objectives and constraints. Essentially, objectives are represented as an objective function which is a mathematical expression that maps the performance criterion to a real number. We utilized it to incorporate the minimum energy representation, desired separation criterion to each other within their group, and the assignment to the final destination (which can also be cast as a constraint if it is a strict requirement). The objective function, unlike constraints, it is not binding. For example, if a group of two pedestrians is walking and an obstacle appears on their path, they have two options. Either they can avoid the obstacle by moving to the same side of the obstacle or split and pass the obstacle from different sides. In the latter case, they will have to break the desired separation criterion (provided in the objective function). This is an approach reflecting reality as it is observed in real life that groups sometimes can split or stay together while tackling obstacles.

Optimization of the designed objective function is subject to the following constraints (a) the path description (initial and final points), (b) the pedestrian dynamical motion, (c) upper and lower bounds on state variables and control input, and (d) obstacles/conflictavoidance constraints.

VI. PROBLEM FORMULATION

In our previous paper [6], we considered a generalized problem of numerous pedestrians transiting an environment with a set of obstacles $\mathcal{O}$. When moving about the environment, the pedestrians walk in a group or individually and show a variety of behavioral patterns. The problem formulation considers pedestrian path planning a group of pedestrians and a pedestrian avoids a stationary obstacle transiting a traffic scenario. However, the problem formulation did not consider conflict avoidance with other moving pedestrians. The modeling framework presented in this paper considers multiple pedestrians or groups of pedestrians transiting through a traffic scenario and avoiding collision with each other.

A self-organized cluster of pedestrians can be mathematically modeled as a moving graph structure $\mathcal{G} = (\mathcal{V}, \mathcal{E})$ where each node v_i in the vertex set $\mathcal{V}$ corresponds to the i^{th} pedestrian in the pedestrian set $\mathcal{P}$. The edge set $\mathcal{E}$ contains links (i, j) between any two pedestrians i and j walking in the same group, each pedestrian aims to uphold specified separation from each other. For each group, $d_{i,j}^{des} = (d_{i,j}^{\parallel des}, d_{i,j}^{\perp des}) \in \mathbb{R}^2$ are the desired lateral and longitudinal separations between any two pedestrians i and j, along the group's path of travel.

The framework associates each pedestrian move through an ordered set of way-points to reach the terminus. For pedestrian i, the next chosen way-point is denoted by w_i. If a pedestrian, at time-step t, is at position $x_{i,t}$ in a global coordinate frame, their direction of travel is indicated by the angle $\theta_i = \angle(w_i - x_{i,t})$. When walking together in a group, it is assumed that all pedestrians possess the same way-point goal. However, we assume here that the goal is adequately far away; thus, the small angle approximations are acceptable for modeling purposes. In other words, $\|\theta_i - \theta_j\| \leq \epsilon$, where ϵ is small, for all pedestrians i and j walking in one group. Table 2 provides a summary of the applicable parameters characterizing the receding horizon control framework for modeling pedestrian movement. More details are provided in our previous paper [6].

Consider Figure 3 illustrating a cluster of pedestrians in the set $\mathcal{P}$. For simplified understanding, we consider two sub-graphs structures $\mathcal{G}_1, \mathcal{G}_2$ in a traffic scene. The sub-graphs are either in line-of-sight or in field-of-view of each other. Within each sub-graphs, pedestrians will maintain their respective private and common objectives. Personal objectives include walking speeds, safe distance to stationery obstacles, conflict avoidance behavioral parameters (Section IV-A), and time-to-arrival. Common objectives are to maintain the moving graph structure discussed previously, which is achieved by preserving the preferred separation between pedestrians in the group. The MILP optimization aims to capture the personal and common objectives along with the dynamic and static constraints associated with pedestrians traveling in the surroundings. The formulation, consisting of the objective functions, associated coefficients, and constraints, when solved, generates an optimal trajectory aligned with the goals and objectives of each pedestrian (and groups). Next, we describe the formulation, decision variables, constraints, and objective functions.

TABLE 2. Description of used parameters.

Symbol	Meaning
$\mathcal{P}$	Set of pedestrians
i	i^{th} pedestrian in the pedestrian set $\mathcal{P}$
j	j^{th} pedestrian in the pedestrian set $\mathcal{P}$
$\mathcal{O}$	Set of obstacles
$\mathcal{F}_o$	Set of facets associated with obstacle o.
$\mathcal{S}_{jk}$	Set of facets associated with pedestrian j at time-step k.
$\mathcal{G} = (\mathcal{V}, \mathcal{E})$	Graph structure defining pedestrian groups.
H_p	Planning horizon [seconds]
H_c	Control horizon [seconds]
$x_{i,t} \in \mathbb{R}^2$	X-Y position of the i^{th} pedestrian at time-step t.
$w_i \in \mathbb{R}^2$	Next way-point of the i^{th} pedestrian.
$\theta_i = \angle(w_i - x_{i,t})$	Direction of travel of i^{th} pedestrian at time-step t.
$d_{i,j}^{des} = (d_{i,j}^{\parallel des}, d_{i,j}^{\perp des}) \in \mathbb{R}^2$	The desired longitudinal and lateral separation between pedestrians i and j along their common direction of travel.

A. DECISION VARIABLES

For a given instantiation of the trajectory planning and execution cycle, each pedestrian i in the pedestrian set $\mathcal{P}$ is foremost characterized according to their current x-y position $x_{i,t_0} \in \mathbb{R}^2$ at time-step t_0 and their preferred next way-point, $w_i \in \mathbb{R}^2$. When optimizing the trajectories for H_p seconds over the planning horizon, it is essential to introduce new decision variables representing each pedestrian's planned position and velocity. To differentiate between the actual position of the pedestrians, $x_{i,t}$, and the planned position of the pedestrians is denoted, $z_{i,k} \forall k \in \{1, \ldots, H_p\}$, representing the position of pedestrian i over H_p seconds when using 1-second increments. We also introduce the decision variables related to the position, velocity, and acceleration of each pedestrian relative to their direction of travel. For clarity, all decision variables described according to the coordinate frame in the direction of travel are indicted by the harpoon accent (e.g., $\overrightarrow{z}_{i,k}$). Therefore, the decision variables for the position, velocity, and acceleration of pedestrian i in the rotated coordinate frame along the direction of travel are presented by $\overrightarrow{z}_{i,k} = (\overrightarrow{z}_{i,k}^{\parallel}, \overrightarrow{z}_{i,k}^{\perp})$,

$\overrightarrow{v}_{i,k} = (\overrightarrow{v}^{\parallel}_{i,k}, \overrightarrow{v}^{\perp}_{i,k})$ and $\overrightarrow{u}_{i,k} = (\overrightarrow{u}^{\parallel}_{i,k}, \overrightarrow{u}^{\perp}_{i,k})$, all defined over $\mathbb{R}^2$ $\forall k \in \{0, \ldots, H_p - 1\}$; each term inside the vectors corresponds to the longitudinal and lateral values along the nominal direction of travel.

The distinction between the position of pedestrians in a global coordinate frame versus a local coordination frame assists in specifying constraints and objective costs related to the position of pedestrians relative to obstacles, other moving pedestrians, and the pedestrians in their group. When forming optimization constraints associated with obstacle/conflict avoidance, it is most straightforward to describe these obstacle constraints using a common global coordinate frame. Meanwhile, because the desired separation between pedestrians walking in a group is described in a relative frame, using a coordinate system aligned with this relative coordinate frame is preferred. Again, velocity and acceleration constraints for every pedestrian are efficiently described in the local coordinate frame. At any time-step, translation of the pedestrian position between the global and a rotated local coordinate frame is provided by the following linear transformation

$$z_{i,k} = R(-\theta_i)\overrightarrow{z}_{i,k} \;\forall\; k \in \{0, \ldots, H_p - 1\} \tag{1}$$

where $R(\theta_i)$ is a rotation matrix

$$R(\theta_i) = \begin{bmatrix} \cos\theta_i & -\sin\theta_i \\ \sin\theta_i & cos\theta_i \end{bmatrix}$$

parameterized by the direction of travel θ_i.

Table 3 provides a list of decision-variables and their descriptions.

B. DYNAMIC CONSTRAINT

One part of the constraint equations represents the dynamic constraints of pedestrian motion. For the i^{th} pedestrian, the second-order discrete-time update equation for their position relative to their direction of travel is given by the following set of constraints

$$\begin{aligned} \overrightarrow{z}_{i,k+1} &= \overrightarrow{z}_{i,k} + \overrightarrow{v}_{i,k}\Delta T + 1/2\overrightarrow{u}_{i,k}\Delta T^2 \\ \overrightarrow{v}_{i,k+1} &= \overrightarrow{v}_{i,k} + \overrightarrow{u}_{i,k}\Delta T \\ \text{and } k &\in \{0, \ldots, H_p - 1\} \end{aligned} \tag{2}$$

Equation (2) adopts a continuously revising process that occurs at a regular time-step of ΔT seconds, during which the acceleration is assumed to be constant.

The pedestrian motion is also constrained by their minimum and maximum walking velocity $(\underline{v}_i, \bar{v}_i)$ and their minimum and maximum acceleration $(\underline{u}_i, \bar{u}_i)$. Assuming that the lateral velocity of pedestrians is small compared to their longitudinal velocity (small angle approximation), we can write

$$\underline{v}_i \leq \overrightarrow{v}^{\parallel}_{i,k} \leq \bar{v}_i \;\forall i \in \mathcal{P}. \tag{3}$$

If the small angle approximation is probable to be violated, it is possible to substitute the velocity constraint in (3) with

$$\left\| \overrightarrow{v}_{i,k} \right\|_2^2 \leq \bar{v}_i \;\forall i \in \mathcal{P}. \tag{4}$$

TABLE 3. Description of decision variables.

Symbol	Meaning
$z_{i,k} \in \mathbb{R}^2$	Planned position of pedestrian i at time-step k in global frame
$z^x_{i,k} \in \mathbb{R}$	x-coordinate of planned position of pedestrian i at time-step k in global frame
$z^y_{i,k} \in \mathbb{R}$	y-coordinate of planned position of pedestrian i at time-step k in global frame
$\overrightarrow{z}_{i,k} = (\overrightarrow{z}^{\parallel}_{i,k}, \overrightarrow{z}^{\perp}_{i,k}) \in \mathbb{R}^2$	Planned position of pedestrian i at time-step k in local frame
$\overrightarrow{v}_{i,k} = (\overrightarrow{v}^{\parallel}_{i,k}, \overrightarrow{v}^{\perp}_{i,k}) \in \mathbb{R}^2$	Planned velocity of pedestrian i at time-step k in local frame
$\overrightarrow{u}_{i,k} = (\overrightarrow{u}^{\parallel}_{i,k}, \overrightarrow{u}^{\perp}_{i,k}) \in \mathbb{R}^2$	Planned acceleration of pedestrian i at time-step k in local frame
$b_{o,f,i,k} \in \{0,1\}$	Binary variable indicating that pedestrian i is outside of the boundary of obstacle o, in reference to facet f of the obstacle, at time-step k
$a_{j,s,i,k} \in \{0,1\}$	Binary variable indicating that pedestrian i is outside of the boundary of the other pedestrian j, in reference to facet s of the pedestrian, at time-step k

Similarly, the acceleration constraints can be given by

$$\left\| \overrightarrow{u}_{i,k} \right\|_2^2 \leq \bar{u}_i \;\forall i \in \mathcal{P}. \tag{5}$$

C. STATIONARY OBSTACLE CONSTRAINT

The obstacle avoidance constraints are inherently non-convex. This can be overcome by using a MILP formulation, where each obstacle avoidance generates binary variables and a set of constraints that correspond to moving *left* or *right* around any obstacle relative to any given side or facet of the obstacle. Consider a convex obstacle o approximated by a polygon defined by a set of f_o facets, $\mathcal{F}_o = \{1, \ldots, f_o\}$; it is possible to define a set of linear constraints

$$h^T_{o,f} y \leq g_{o,f} \;\forall f \in \mathcal{F}_o \tag{6}$$

that represent half-spaces used to define the set of points in space, $y \in \mathbb{R}^2$, that are blocked by the obstacle. Here, for each side or facet of a polygon, the vector $h_{o,f}$ corresponds to the vector normal to the facet f, while $g_{o,f}$ is allowable projected offset off the facet.

For obstacle avoidance, the planned position of a pedestrian, $z_{i,k}$, must be outside the convex polygon at each time. The i^{th} pedestrian is outside of the obstacle o (with respect to a single facet $f \in \mathcal{F}_o$), if their position at time-step k satisfies the constraint

$$g_{o,f} - h^T_{o,f} x_{i,k} \leq 0 \tag{7}$$

Therefore, to dodge obstacle o, (7) must hold for at least one of the facets f. The manifestation of such a

constraint is composed as

$$\begin{cases} g_{o,1} - h_{o,1}^T x_{i,k}, \ \leq 0 \\ or \\ \vdots \\ or \\ g_{o,f} - h_{o,f}^T x_{i,k}, \ \leq 0 \\ or \\ \vdots \\ or \\ g_{o,F} - h_{o,F}^T x_{i,k}, \ \leq 0. \end{cases} \tag{8}$$

Implementation of the constraint in (8) can be achieved using Big-M notation within a MILP solver by introducing binary variables $b_{o,f,i,k} \in \{0, 1\}\ \forall f \in \mathcal{F}\ and\ k \in \{1, \ldots, H_p\}$. Here the binary logical condition $b_{o,f,i,k} = 1$ indicates that pedestrian i is evading obstacle o at time-step k relative to facet f. This is implemented for all pedestrians and all obstacles using the following constraint equations:

$$\begin{aligned} & g_{o,f} - h_{o,f}^T x_{i,k} \leq M\big(1 - b_{o,f,i,k}\big)\ \forall f \in \mathcal{F}_o, o \in \mathcal{O} \\ & i \in \mathcal{P}, k \in \big\{1, \ldots, H_p\big\} \\ & \sum_{f \in \mathcal{F}_o} b_{o,f,i,k} \geq 1\ \forall o \in \mathcal{O}, i \in \mathcal{P} \\ & k \in \big\{1, \ldots, H_p\big\} \end{aligned} \tag{9}$$

where M is sufficiently large such that the f^{th} constraint holds when $b_{o,f} = 0$ regardless of the pedestrian's position.

A buffer distance can be added around each obstacle that can work as a buffer of comfort distance. Any extra buffer distance, $e_{o,i}$, depends on the specific obstacle o and pedestrian i; in this case, each obstacle constraint can be adjusted to

$$g_{o,f} - h_{o,f}^T x_{i,k} \leq -\big\|h_{o,f}\big\| e_{o,i}. \tag{10}$$

D. CONFLICT AVOIDANCE CONSTRAINT

The potential presence of moving obstacles (e.g., other pedestrians) within the surroundings requires pedestrians to plan their trajectories accordingly. One approach for collision avoidance is similar to stationary obstacle avoidance, using inherently non-convex constraints. The non-convexity challenge can be mitigated by using binary variables and a set of constraints that correspond to moving *left* or *right* around the other pedestrian relative to any given side. In order to avoid collision with other moving pedestrians, the pedestrian tries to maintain certain safety/comfort distances with them in each direction at every time-step. Section IV illustrated how safety/comfort distances would depend from case to case in the chosen case scenarios. However, for the sake of simplicity, we assume that at time-step k, j^{th} pedestrian can be represented by a polygon with a set of facets, $\mathcal{S}_{jk} = \{1, \ldots, S_j\}$. For conflict avoidance, the planned position of another pedestrian i at any point in time, $z_{i,k}$, must be outside the approximated convex polygon. The i^{th} pedestrian avoids collision with j if their position at time-step k satisfies the constraint

$$g_{j,s} - h_{j,s}^T x_{i,k} \leq 0 \tag{11}$$

Note that conflict avoidance is about a single facet $s \in \mathcal{S}_{jk}$ of the polygon representing pedestrian j at time-step k. Accordingly, to avoid the collision, (11) must hold for at least one of the facets s at every time-step k. The manifestation of such a constraint is given as

$$\begin{cases} g_{j,1} - h_{j,1}^T x_{i,k}, \leq 0 \\ or \\ \vdots \\ or \\ g_{j,s} - h_{j,s}^T x_{i,k}, \ \leq 0 \\ or \\ \vdots \\ or \\ g_{j,S} - h_{j,S}^T x_{i,k}, \leq 0. \end{cases} \tag{12}$$

Implementation of the constraint in (12) can be achieved using Big-M notation within a MILP solver after introducing binary variables $a_{j,s,i,k} \in \{0, 1\}\ \forall s \in \mathcal{S}\ and\ k \in \{1, \ldots, H_p\}$. Here the binary logical condition $a_{j,s,i,k} = 1$ indicates that pedestrian i avoids a collision with pedestrian j at time-step k relative to facet s. This can be implemented for all pedestrians using the following constraint equations:

$$\begin{aligned} & g_{j,s} - h_{j,s}^T x_{i,k} \leq L\big(1 - a_{j,s,i,k}\big)\ \forall s \in \mathcal{S}_{jk}, j \in \mathcal{P} \\ & i \in \mathcal{P}, k \in \big\{1, \ldots, H_p\big\} \\ & \sum_{s \in \mathcal{S}_{jk}} a_{j,s,i,k} \geq 1\ \forall j \in \mathcal{P}, i \in \mathcal{P} \\ & k \in \big\{1, \ldots, H_p\big\} \end{aligned} \tag{13}$$

where L is large enough such that the s^{th} constraint holds when $a_{j,s} = 0$ regardless of the pedestrian's position. For practical purposes, the value of L can be set based on the dimensions of the environment.

E. PRIVATE AND COMMON OBJECTIVE FUNCTIONS

Pedestrians seek personal objectives (e.g., minimization of their effort, minimizing travel time) as well as global goals shared with other pedestrians (e.g., maintaining the desired formation) [24], [40], [41], [42]. Therefore, we have formulated a generalizable objective function taking into account all these aspects.

1) PERSONAL OBJECTIVES

The personal or private objective function can account for regulating walking speeds, running costs, and the terminal cost of reaching the desired way-point.

$$\begin{aligned} \sum_{k=1}^{H_p} \sum_{i \in \mathcal{P}} \Big(& k_i^{acc} \big\| u_{i,k} - u_i^{des} \big\| + k_i^{speed} \big\| v_{i,k} - v_i^{des} \big\| \\ & + k_i^{run} \big\| x_{i,k} - w_i \big\| \Big) \\ & + \sum_{i \in \mathcal{P}} k_i^{term} \big\| x_{i,H_p} - w_i \big\| \end{aligned} \tag{14}$$

TABLE 4. Short-hand markers indicating the ranges over which constraints apply.

Sets	Short-hand notation
$i \in \mathcal{P}, k \in \{1, \ldots, H_p\}$	⊛
$i \in \mathcal{P}, k \in \{0, \ldots, H_p - 1\}$	•
$i \in \mathcal{P}, k \in \{0, \ldots, H_p\}$	♦
$i \in \mathcal{P}, k \in \{1, \ldots, H_p\}, o \in \mathcal{O}, f \in \mathcal{F}_o$	▲
$i \in \mathcal{P}, k \in \{1, \ldots, H_p\}, o \in \mathcal{O}$	†
$i, j \in \mathcal{P}, k \in \{1, \ldots, H_p\}, s \in \mathcal{S}_{jk}$	♣
$i, j \in \mathcal{P}, k \in \{1, \ldots, H_p\}$	♠

In the personal objective costs described above, each norm can be adapted according to chosen modeling (i.e., ℓ_1, ℓ_2, or ℓ_∞). Further, the weights can be adjusted to reflect their relative importance.

2) COMMON OBJECTIVES

Desired Formation: When walking as part of a group, pedestrians can optimize their planned trajectories while maintaining the desired formation. It is achieved by penalizing any divergences between the actual and desired separation. The following objective function can achieve it:

$$\sum_{k=1}^{H_p} \sum_{(i,j)\in\mathcal{E}} k_{i,j}^{sep} \left\| \overrightarrow{z}_{i,k} - \overrightarrow{z}_{j,k} - d_{i,j}^{des} \right\| \tag{15}$$

Note that the summation over the edge-set $\mathcal{E}$ in the graph structure $\mathcal{G}$ provides for considerable flexibility. For instance, ensuring consistency in the desired separation between pedestrians is unnecessary. So for any three pedestrians h, i, and j in the same pedestrian group there is no necessity that $d_{i,j}^{des} + d_{j,h}^{des} = d_{i,h}^{des}$. Pedestrians in the same group don't need to seek to maintain the desired separation.

Special Cases: In typical cases (e.g., a parent and child are walking together), it may be more suitable to represent separation distances within constraints instead of within objective costs. When two pedestrians must remain within a specified range $r_{i,j}$ of each other, the comparable convex constraint is expressed as

$$\left\| \overrightarrow{z}_{i,k} - \overrightarrow{z}_{j,k} \right\| \leq r_{i,j} \;\forall\; k \in \{1, \ldots, H_p\} \tag{16}$$

F. MODEL SUMMARY

A summary of the entire formulation is mentioned next. Table 4 provides a short-hand notation to indicate the ranges for which each of the constraints holds. For instance, all equations that hold true over $i \in \mathcal{P}, k \in \{1, \ldots, H_p - 1\}$ are indicted by the • symbol. Note that all decision variables mentioned in the summary are considered to be unrestricted, barring any binary variables. Also, to preserve generality, we abstain from specifying which norm is used in the objective function and constraints. While the ℓ_2 norm is suitable in many cases, representations using the ℓ_1 or ℓ_∞ are also acceptable.

$$\begin{aligned}
\min \sum_{k=1}^{H_p} \sum_{i\in\mathcal{P}} \Big(& k_i^{acc} \left\| u_{i,k} - u_i^{des} \right\| \\
& + k_i^{speed} \left\| v_{i,k} - v_i^{des} \right\| \\
& + k_i^{pos} \left\| x_{i,k} - w_i \right\| \Big) \\
& + \sum_{i\in\mathcal{P}} k_i^{term} \left\| x_{i,H_p} - w_i \right\| \\
& + \sum_{k=1}^{H_p} \sum_{(i,j)\in\mathcal{E}} k_{i,j}^{sep} \left\| \overrightarrow{z}_{i,k} - \overrightarrow{z}_{j,k} - d_{i,j}^{des} \right\| \\
s.t. \quad & \overrightarrow{z}_{i,k+1} = \overrightarrow{z}_{i,k} + \overrightarrow{v}_{i,k}\Delta T + 1/2\,\overrightarrow{u}_{i,k}\Delta T^2 && \bullet \\
& \overrightarrow{v}_{i,k+1} = \overrightarrow{v}_{i,k} + \overrightarrow{u}_{i,k}\Delta T && \bullet \\
& \left\| \overrightarrow{v}_{i,k} \right\| \leq \bar{v}_i && ⊛ \\
& \left\| \overrightarrow{u}_{i,k} \right\| \leq \bar{u}_i && ⊛ \\
& z_{i,k} = R(-\theta_i)\,\overrightarrow{z}_{i,k} && ♦ \\
& g_{o,f} - h_{o,f}^T x_{i,k} \leq M\big(1 - b_{o,f,i,k}\big) && ▲ \\
& \sum_{f\in\mathcal{F}_o} b_{o,f,i,k} \geq 1 && † \\
& b_{o,f,i,k} \in \{0, 1\} && ▲ \\
& g_{j,s} - h_{j,s}^T x_{i,k} \leq L\big(1 - a_{j,s,i,k}\big) && ♣ \\
& \sum_{s\in\mathcal{S}_{jk}} a_{j,s,i,k} \geq 1 && ♠ \\
& a_{j,s,i,k} \in \{0, 1\} && ♣
\end{aligned}$$

G. IMPLEMENTATION DETAILS

`MATLAB` along with the `CVX` optimization library was used to implement the receding-horizon framework with the embedded MILP [43].

The proposed generative framework is implemented to show the model performance for non-linear conflict avoidance (human-human) traffic scenarios. The model can implement various interacting traffic scenarios. To validate the model performance for social interaction traffic scenarios, we identified the case studies where the agents move towards each other - directly or indirectly (more details in Section IV). The identified case studies are capable of manifesting the most common moving human-human conflict avoidance case scenarios. We have previously defined the safety distances (d_1^{ILS}, d_2^{ILS}, d_1^{IFV}, d_2^{IFV}, etc.) that pedestrian tries to maintain with other moving pedestrian. For simplicity in implementation, we approximate the scenario parameters described in Table 1 with an exclusion zone as a square with each side of d_c units.

VII. EXPERIMENT DETAILS

A. DATA DESCRIPTION

There are two datasets used in this paper. The DUT dataset [44] is used to calibrate the proposed model and

TABLE 5. Calibrated model parameters.

Parameters	Calibrated Values
$d_{i,j}^{\perp des}$	$\mu = 0.52, \sigma = 0.15$
$d_{i,j}^{\parallel des}$	$\mu = 0.097, \sigma = 0.046$
Average minimum velocity	0.97 m/sec
Average maximum velocity	1.70 m/sec
Average minimum acceleration	-0.3 m/sec^2
Average maximum acceleration	0.3 m/sec^2

validate its efficiency. And the TrajNet++ dataset [32] is used to cross-validate the generalizability of the model. The DUT dataset is one of the crowd interaction benchmark datasets [44] collected at the campus of Dalian University of Technology (DUT) in China. The videos were recorded using the *DJI Mavic Pro* Drone with a down-facing camera. The video resolution was 1920×1080 with an *fps* of 23.98. Pedestrians in the data are mainly college students. The pedestrian trajectories were extracted from the recorded video data using video stabilization and filtering techniques. The TrajNet++ is an interaction-centric human trajectory forecasting benchmark [32]. It comprises largely of human social interactions and traffic scenarios from various human trajectory datasets.

B. MODEL PARAMETERS AND CALIBRATION

Model Parameters: The key parameters used in the model are:

1) Total time-steps for a simulation (T)
2) Desired longitudinal distance between pedestrians i and j ($d_{i,j}^{\parallel des}$)
3) Desired lateral distance between pedestrians i and j ($d_{i,j}^{\perp des}$)
4) Control Horizon (H_c)
5) Planning Horizon (H_p)
6) Maximum and Minimum mean velocity
7) Maximum and Minimum mean acceleration.

Calibration: The model key parameters are calibrated by identifying the interacting conflict avoidance traffic scenarios in the datasets. The key model parameters (numbered 2 to 7 in Section VII-B) are taken from our previous work [6]. The d_c is calibrated based on traffic scenarios observations. The pedestrian maintain a behavioral safe distance in order to avoid collision. The sampling time T depends on the considered traffic scenario. We extracted fifty samples from the dataset, thirty-five samples are used for training the model and fifteen samples used for testing the developed model. The $d_{i,j}^{\perp des}$ and $d_{i,j}^{\parallel des}$ values are dynamically calibrated using the normal distribution method. The calibrated parameters are shown in Table 5.

C. PERFORMANCE METRICS

We use the following performance metrics.

- MED: Mean Euclidean Distance is the average Euclidean distance between the model predicted coordinates and the actual coordinates of the pedestrian at every instant. Lower is better.
- FDE: Final Displacement Error is the Euclidean distance between the model predicted final destination and the actual final destination at the corresponding time instant.

VIII. EXPERIMENTAL RESULTS

To validate the model we identify the case studies, as listed in Section IV, from the datasets. The calibrated model is provided with required input states and then the model generates pedestrian trajectories for the traffic scenario. The chosen case studies are where pedestrians are moving towards each other directly (considered as line-of-sight conflict avoidance) or indirectly (considered as field-of-view conflict avoidance). Note that the trajectory generative framework is generalizable and can generate pedestrian trajectories across a broad range of pedestrian scenarios.

Simulation Results and Discussion: The experimental results demonstrate the capability and efficiency of the HISS framework. Figure 5, Figure 6, and Figure 7 demonstrates the trajectory generation results. We have taken fifty samples of each chosen case study. The samples are divided into a ratio of seventy and thirty for calibration and validation, respectively. The calibrated values for all case studies are in Table 5. The calibrated values are used depending on the case study; if it has the group of people walking together and avoiding the collision with an individual or another group, $d_{i,j}^{\perp des}$ and $d_{i,j}^{\parallel des}$ values are also used in the model implementation. The average velocity and acceleration values in the calibration table work equally well for all the case studies.

Figure 5a shows the screenshot from the DUT dataset in which pedestrians number 5 and 36 are in each other's line-of-sight; the two pedestrians adjusted their trajectories to avoid the collision. Figure 5b shows the model generated trajectory for the same set of pedestrians. The solid color lines are the real trajectories of pedestrians 5 and 36, and the dashed lines are model generated trajectories. Due to the utilization of behavioral and social interaction rules, the model is successfully generating trajectories that are similar to real trajectories for the given scenarios. A similar explanation for the other shown case studies results. Figure 8 and Figure 9 show the values of the MED and FDE for the respective case studies samples performed for model validation. Table 6 shows the chosen case studies' performance metrics - mean Euclidean distance (MED) and final displacement error (FDE) values. The performance metrics have low values, which supports the model's efficiency in generating realistic trajectories for given scenarios. The FDE values are close to one, the reason is firstly, the performance metrics values are the average values of thirty test samples, and also, we are using the average values of velocity, which can differ from sample to sample, and therefore for some samples, it might be some difference in reaching the final position. It is observed that MED values are near zero for the case

(a) Screenshot of Agent 5 and Agent 36 avoiding line-of-sight collision

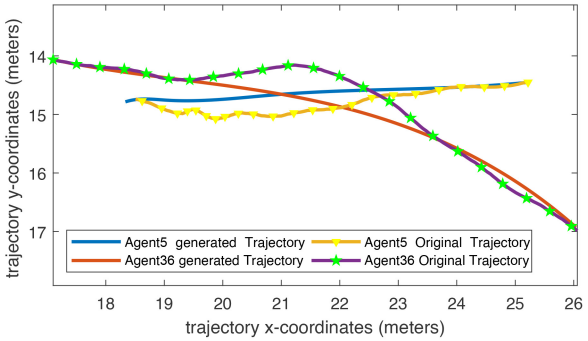

(b) Agent 5 and Agent 36's Actual trajectory and Model generated trajectories

FIGURE 5. Line-of-sight Collision Avoidance - Individual.

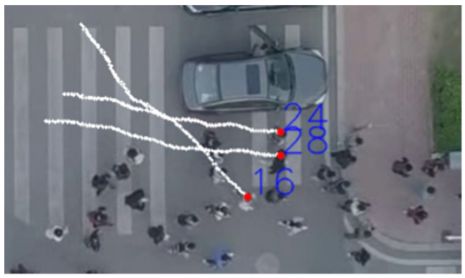

(a) Screenshot of Agent 16 avoiding collision with the group of two pedestrians 24 and 28

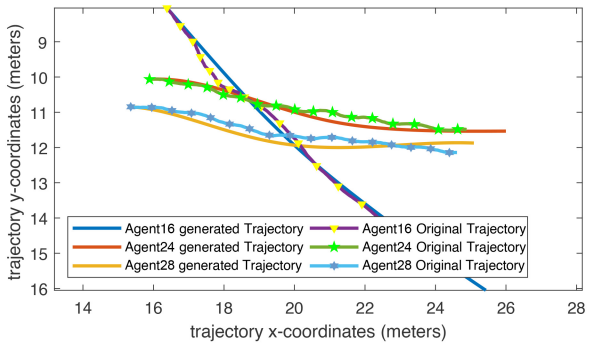

(b) Agent 16, Agent 24 and Agent 28 - Actual trajectory and Model generated trajectories

FIGURE 6. Field-of-view Collision Avoidance - Group.

(a) Screenshot from DUT dataset showing Agent 9 and Agent 10 avoiding collision

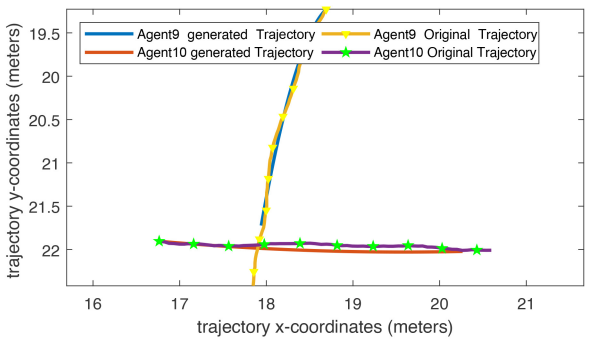

(b) Actual and Model generated trajectories of Agent 9 and Agent 10

FIGURE 7. Field-of-View Collision Avoidance - Individual.

studies, which implies that generated trajectories are close to realistic trajectories.

Baseline Comparison: The comparison with existing trajectory generation frameworks is presented in this section. The proposed framework lies between the two sets of modeling paradigms — the black-box algorithms (such as machine learning), which are hard to interpret and parameterize, and the analytical modeling with a set of parameterized equations. There are some well-known traditional models, such as Social Force and Cellular Automata models; these models are non-black-box and are parameterized; however, such models' code availability is an issue, and even the used datasets are not openly available. Moreover, these models are not designed for pedestrians group behaviors. The comparison with the black box algorithm (such as machine learning algorithms) for trajectory generation, ideally, is also not suitable to be considered baselines for comparison with the proposed model. The black-box models are mainly predictive models which predict trajectories for the near future using past observations. The proposed pedestrian trajectory model

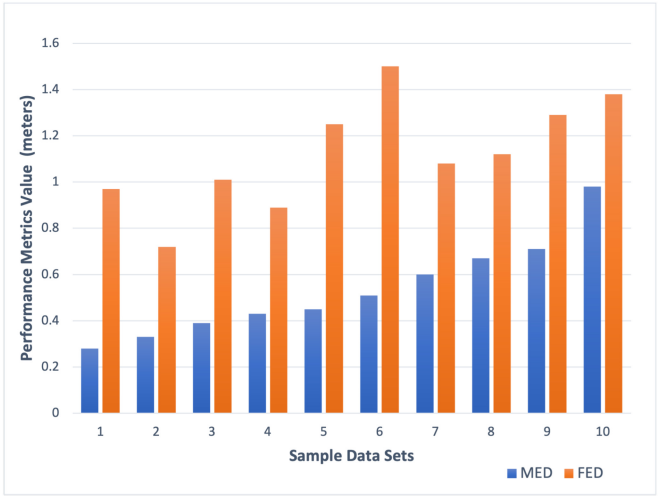

FIGURE 8. Performance Metrics Average Values of Case Study 'Line-of-sight Conflict Avoidance-Individual.'

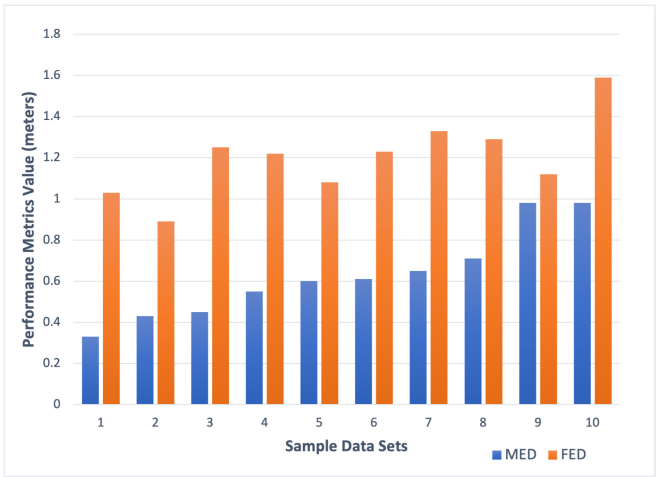

FIGURE 9. Performance Metrics Average Values of Case Study 'Field-of-view Conflict Avoidance-Group.'

is a generative model which is fully defined and parameterized with pedestrians' behavioral and interaction rules. The cost function and constraints for a given scenario are not only observable but can also be easily modified to reflect different scenarios of pedestrian movements and interactions. Thus, it is important to note that a direct comprehensive comparison with the state-of-the-art is not possible. Table 7 compares the MED and FED for state-of-the-art models and our algorithm in the three scenarios using the TrajNet++ dataset. Note that the proposed approach has comparable (or even better) error metrics. However, the comparison table should be interpreted subjectively since, as we stated earlier, the model goals are not aligned.

Cross Validation: TrajNet++ is an interaction-centric trajectory dataset [32]. We have used TrajNet++ to cross-validate HISS framework. The idea is to validate the generalizability of the proposed framework. That is to say, the model parameters trained on the DUT dataset will still

TABLE 6. Performance metrics table for simulated traffic scenarios on DUT dataset.

Experimental Results using DUT dataset (HISS Framework)	Performance Metrics(meters)	
	MED	FDE
Line-of-sight Conflict Avoidance - Individual	0.54	1.13
Field-of-view Conflict Avoidance - Group	0.63	1.21
Field-of-View Conflict Avoidance- Individual	0.53	0.98

TABLE 7. Performance metrics comparison chart for different pedestrian trajectory forecasting models.

Comparison with State-of-the-art models (TrajNet++ dataset)	Performance Metrics (meters)	
	MED	FDE
PecNet [45][46]	0.57	1.18
AIN [47] [46]	0.62	1.24
Social NCE [48] [46]	0.53	1.14
AMENet [49] [46]	0.62	1.30

TABLE 8. Cross validation using TrajNet++ datasets.

Cross-validation Results for (TrajNet++ dataset)	Performance Metrics (meters)	
	MED	FDE
Line-of-sight Conflict Avoidance - Individual	0.66	1.10
Field-of-View Conflict Avoidance- Individual	0.55	1.05

perform well on the TrajNet++ dataset. Table 8 shows the calculated performance metrics using the estimated parameters from DUT dataset and using them to generate TrajNet++ conflict avoidance scenarios. The evaluation metrics in the table have values of less than one, which demonstrates the good performance of the approach.

IX. CONCLUSION AND FUTURE RESEARCH DIRECTION

The paper proposed a receding horizon optimization-based pedestrian trajectory generation framework that generates the pedestrian trajectory by planning and updating the trajectory for every next few time steps in the presence of various traffic interactions. The HISS framework has utilized pedestrians' conflict avoidance scenario-specific behavioral and social interaction rules. In this research, more specifically, the framework has incorporated the conflict avoidance with moving obstacles - one of the significant behavioral studies and composes most pedestrian traffic scenarios. The model validation experiments were performed for the chosen traffic scenarios on the two publicly available real datasets. The performance metrics - MED has near zero values, and FDE has close to one value validating the effectiveness of the proposed pedestrian trajectory generation framework.

The proposed framework is parameterized and capable of incorporating any traffic scenario-specific behavioral rules. The framework could serve as a good simulation tool

to urban planners and modelers because of its simplicity of design and yet good accuracy. The model is capable of fine-grained implementation of pedestrian behavior and interaction to explore different pedestrian movement scenario for a given shared space scenario. The proposed framework exhibits the feature of both explanatory and predictive modeling approaches. When programmed to plausible pedestrian behavior and interactions, the framework produces trajectories with patterns to those observable in real-world traffic scenarios, justifying the framework's capability to provide explanations and solutions to various traffic situations in the real world. Now, the predictive feature of the proposed model is such that the model assesses the current information available about the traffic scene and predicts the trajectory for the next few time steps. This way, the model generates the trajectories as a human does, i.e., by accessing the traffic scenario at every time step and updating the trajectory based on the assessment. The inclusion of explanatory and prediction features makes the proposed pedestrian trajectory generation framework a very powerful tool and will be useful for urban city planners and modelers in making policy decisions for urban city planning.

One of the limitations of the study is that we approximated the convex polygon as a square for implementation convenience. A more general representation of the stationary and moving obstacles may be considered in the future studies. Also, although the HISS framework can incorporate pedestrian-vehicle or pedestrian-active mobility agent interactions, the case studies did not evaluate them. The future work should consider to extend the proposed framework to cyclist and other micromobility modes.

REFERENCES

[1] B. Hamilton-Baillie, "Shared space: Reconciling people, places and traffic," *Built Environ.*, vol. 34, no. 2, pp. 161–181, 2008.

[2] B. C. Tefft, L. S. Arnold, and W. J. Horrey, *Examining the Increase in Pedestrian Fatalities in the United States, 2009–2018 (Research Brief)*, AAA Found. Traffic Saf., Washington, DC, USA, 2021. Accessed: Nov. 22, 2021.

[3] "Pedestrian traffic fatalities by state: 2019 preliminary data," GHSA, Washington, DC, USA, GHSA Annu. Spotlight Rep., 2020. Accessed: Nov. 22, 2021. [Online]. Available: https://www.ghsa.org/resources/Pedestrians20

[4] S. P. Hoogendoorn and P. H. L. Bovy, "Normative pedestrian behaviour theory and modelling," in *Transportation and Traffic Theory in the 21st Century*. Bingley, U.K.: Emerald Group Publ. Ltd., 2002.

[5] S. Hoogendoorn and P. H. L. Bovy, "Gas-kinetic modeling and simulation of pedestrian flows," *Transp. Res. Rec. J. Transp. Res. Board*, vol. 1710, no. 1, pp. 28–36, 2000.

[6] S. Gupta, M. H. Zaki, and A. Vela, "Generative modeling of pedestrian behavior: A receding horizon optimization-based trajectory planning approach," *IEEE Access*, vol. 10, pp. 81624–81641, 2022.

[7] A. Bemporad and M. Morari, "Control of systems integrating logic, dynamics, and constraints," *Automatica*, vol. 35, no. 3, pp. 407–427, 1999.

[8] H. P. Williams and S. C. Brailsford, "Computational logic and integer programming," in *Advances in Linear and Integer Programming*, vol. 4. Oxford, U.K.: Oxford Univ. Press, 1996, pp. 249–281.

[9] A. Nayak, A. Eskandarian, and Z. Doerzaph, "Uncertainty estimation of pedestrian future trajectory using Bayesian approximation," 2022, *arXiv:2205.01887*.

[10] L. Wang, W. Hu, and T. Tan, "Recent developments in human motion analysis," *Pattern Recognit.*, vol. 36, no. 3, pp. 585–601, 2003.

[11] G. Solmaz and D. Turgut, "A survey of human mobility models," *IEEE Access*, vol. 7, pp. 125711–125731, 2019.

[12] T. B. Moeslund, A. Hilton, and V. Krüger, "A survey of advances in vision-based human motion capture and analysis," *Comput. Vis. Image Understand.*, vol. 104, nos. 2–3, pp. 90–126, 2006.

[13] D. Helbing and P. Molnar, "Social force model for pedestrian dynamics," *Phys. Rev. E, Stat. Phys. Plasmas Fluids Relat. Interdiscip. Top.*, vol. 51, no. 5, pp. 4282–4286, 1995.

[14] V. J. Blue and J. L. Adler, "Emergent fundamental pedestrian flows from cellular automata microsimulation," *Transp. Res. Rec. J. Transp. Res. Board*, vol. 1644, no. 1, pp. 29–36, 1998.

[15] D. C. Duives, W. Daamen, and S. P. Hoogendoorn, "State-of-the-art crowd motion simulation models," *Transp. Res. C, Emerg. Technol.*, vol. 37, pp. 193–209, Dec. 2013.

[16] S. Wolfram et al., *A New Kind of Science*, vol. 5. Champaign, IL, USA: Wolfram Media, 2002.

[17] D. C. Parker, S. M. Manson, M. A. Janssen, M. J. Hoffmann, and P. Deadman, "Multi-agent systems for the simulation of land-use and land-cover change: A review," *Ann. Assoc. Amer. Geograph.*, vol. 93, no. 2, pp. 314–337, 2003.

[18] C. J. Castle and A. T. Crooks, *Principles and Concepts of Agent-Based Modelling for Developing Geospatial Simulations*, Univ. Coll. London, London, U.K., 2006.

[19] N. Cetin, K. Nagel, B. Raney, and A. Voellmy, "Large-scale multi-agent transportation simulations," *Comput. Phys. Commun.*, vol. 147, nos. 1–2, pp. 559–564, 2002.

[20] D. Helbing, *Social Self-Organization: Agent-Based Simulations and Experiments to Study Emergent Social Behavior*. Berlin, Germany: Springer, 2012. [Online]. Available: https://link.springer.com/book/10.1007/978-3-642-24004-1#about-this-book

[21] M. Hussein and T. Sayed, "A bi-directional agent-based pedestrian microscopic model," *Transportmetrica A, Transport Sci.*, vol. 13, no. 4, pp. 326–355, 2017.

[22] A. Crooks, C. Castle, and M. Batty, "Key challenges in agent-based modelling for geo-spatial simulation," *Comput. Environ. Urban Syst.*, vol. 32, no. 6, pp. 417–430, 2008.

[23] R. Alsaleh and T. Sayed, "Modeling pedestrian-cyclist interactions in shared space using inverse reinforcement learning," *Transp. Res. F, Traffic Psychol. Behav.*, vol. 70, pp. 37–57, Apr. 2020.

[24] M. Moussa'ıd, N. Perozo, S. Garnier, D. Helbing, and G. Theraulaz, "The walking behaviour of pedestrian social groups and its impact on crowd dynamics," *PLoS One*, vol. 5, no. 4, 2010, Art. no. e10047.

[25] M. Moussa'ıd, D. Helbing, and G. Theraulaz, "How simple rules determine pedestrian behavior and crowd disasters," *Proc. Nat. Acad. Sci.*, vol. 108, no. 17, pp. 6884–6888, 2011.

[26] M. H. Zaki and T. Sayed, "Automated classification of road-user movement trajectories," *Transp. Res. C, Emerg. Technol.*, vol. 33, pp. 50–73, Aug. 2013.

[27] M. Seitz, G. Köster, and A. Pfaffinger, "Pedestrian group behavior in a cellular automaton," in *Pedestrian and Evacuation Dynamics 2012*. Cham, Switzerland: Springer, 2014, pp. 807–814.

[28] D. Ridel, E. Rehder, M. Lauer, C. Stiller, and D. Wolf, "A literature review on the prediction of pedestrian behavior in urban scenarios," in *Proc. 21st Int. Conf. Intell. Transp. Syst. (ITSC)*, 2018, pp. 3105–3112.

[29] M. H. Zaki and T. Sayed, "Automated analysis of pedestrian group behavior in urban settings," *IEEE Trans. Intell. Transp. Syst.*, vol. 19, no. 6, pp. 1880–1889, Jun. 2018.

[30] V. Papathanasopoulou, I. Spyropoulou, H. Perakis, V. Gikas, and E. Andrikopoulou, "A data-driven model for pedestrian behavior classification and trajectory prediction," *IEEE Open J. Intell. Transp. Syst.*, vol. 3, pp. 328–339, 2022.

[31] S. Zhang and M. Abdel-Aty, "Real-time pedestrian conflict prediction model at the signal cycle level using machine learning models," *IEEE Open J. Intell. Transp. Syst.*, vol. 3, pp. 176–186, 2022.

[32] P. Kothari, S. Kreiss, and A. Alahi, "Human trajectory forecasting in crowds: A deep learning perspective," *IEEE Trans. Intell. Transp. Syst.*, vol. 23, no. 7, pp. 7386–7400, Jul. 2022.

[33] C. Vater, B. Wolfe, and R. Rosenholtz, "Peripheral vision in real-world tasks: A systematic review," *Psychonomic Bull. Rev.*, vol. 29, no. 5, pp. 1531–1557, 2022. [Online]. Available: https://link.springer.com/article/10.3758/s13423-022-02117-w

[34] A. H. Gloriani and A. C. Schütz, "Humans trust central vision more than peripheral vision even in the dark," *Current Biol.*, vol. 29, no. 7, pp. 1206–1210, 2019.
[35] A. Gasparetto, P. Boscariol, A. Lanzutti, and R. Vidoni, "Path planning and trajectory planning algorithms: A general overview," in *Motion Operation Planning of Robotic Systems*. Cham, Switzerland: Springer, 2015, pp. 3–27.
[36] A. Gasparetto, P. Boscariol, A. Lanzutti, and R. Vidoni, "Trajectory planning in robotics," *Math. Comput. Sci.*, vol. 6, no. 3, pp. 269–279, 2012.
[37] N. Neef, K. Kastner, M. Schmidt, and S. Schmidt, "On Optimizing driving patterns of autonomous cargo bikes as a function of distance and speed—A psychological study," *IEEE Open J. Intell. Transp. Syst.*, vol. 3, pp. 592–601, 2022.
[38] D. Verscheure, B. Demeulenaere, J. Swevers, J. De Schutter, and M. Diehl, "Time-energy optimal path tracking for robots: A numerically efficient optimization approach," in *Proc. 10th IEEE Int. Workshop Adv. Motion Control*, 2008, pp. 727–732.
[39] H. Xu, J. Zhuang, Z. Zhu, and S. Wang, "Global time-energy optimal planning of robot trajectories," in *Proc. Int. Conf. Mechatronics Autom.*, 2009, pp. 4034–4039.
[40] W. Ge, R. T. Collins, and R. B. Ruback, "Vision-based analysis of small groups in pedestrian crowds," *IEEE Trans. Pattern Anal. Mach. Intell.*, vol. 34, no. 5, pp. 1003–1016, May 2012.
[41] W. Daamen and S. P. Hoogendoorn, "Experimental research of pedestrian walking behavior," *Transp. Res. Rec. J. Transp. Res. Board*, vol. 1828, no. 1, pp. 20–30, 2003.
[42] J. Drury, C. Cocking, and S. Reicher, "Everyone for themselves? a comparative study of crowd solidarity among emergency survivors," *Brit. J. Soc. Psychol.*, vol. 48, no. 3, pp. 487–506, 2009.
[43] M. Grant and S. Boyd. "CVX: MATLAB software for disciplined convex programming, version 2.1." Mar. 2014. [Online]. Available: http://cvxr.com/cvx
[44] D. Yang, L. Li, K. Redmill, and Ü. Özgüner, "Top-view trajectories: A pedestrian dataset of vehicle-crowd interaction from controlled experiments and crowded campus," in *Proc. IEEE Intell. Veh. Symp. (IV)*, 2019, pp. 899–904.
[45] K. Mangalam et al., "It is not the journey but the destination: Endpoint conditioned trajectory prediction," in *Proc. Eur. Conf. Comput. Vis.*, 2020, pp. 759–776.
[46] R. Rozenberg, J. Gesnouin, and F. Moutarde, "Asymmetrical Bi-RNN for pedestrian trajectory encoding," 2021, *arXiv:2106.04419*.
[47] Y. Zhu, D. Ren, M. Fan, D. Qian, X. Li, and H. Xia, "Robust trajectory forecasting for multiple intelligent agents in dynamic scene," 2020, *arXiv:2005.13133*.
[48] Y. Liu, Q. Yan, and A. Alahi, "Social NCE: Contrastive learning of socially-aware motion representations," in *Proc. IEEE/CVF Int. Conf. Comput. Vis.*, 2021, pp. 15118–15129.
[49] H. Cheng, W. Liao, M. Y. Yang, B. Rosenhahn, and M. Sester, "AMENet: Attentive maps encoder network for trajectory prediction," *ISPRS J. Photogrammetry Remote Sens.*, vol. 172, pp. 253–266, Jan. 2021.

SAUMYA GUPTA received the B.S. degree in electronics and instrumentation engineering from U.P. Technical University, India, the M.S. degree in electrical engineering from the University of Nevada Las Vegas (UNLV), and the Doctoral degree in civil engineering from the University of Central Florida in Fall 2022. During her tenure at UNLV from 2014 to 2016, she served as a Research Assistant with Transportation Research Center. She later joined PolyPak America, Los Angeles, California, as a Data Scientist from 2016 to 2018. Concurrently, she contributed her expertise as an Adjunct Professor of Electrical Engineering with California State University Los Angeles from 2017 to 2018. In addition to her academic and professional pursuits, she also gained experience as a sustainability intern with Orange County Government, FL, USA, from May 2022 to November 2022. This role provided her with valuable insights into the implementation of sustainable practices within a governmental context. Her research interests revolve around optimization, modeling and simulation, active mobility, pedestrian behavior and interactions, urban planning, and sustainability.

MOHAMED H. ZAKI (Member, IEEE) received the Doctoral degree from Hardware Verification Group, Concordia University, Montreal, in 2008. He is an Assistant Professor with the Civil and Environmental Engineering Department, Western University, Ontario. Till 2022, he was an Assistant Professor with the Civil, Environmental and Construction Engineering Department, University of Central Florida. Before, he was a Research Associate with the Bureau of Intelligent Transportation Systems and Freight Security, The University of British Columbia. His multidisciplinary research focuses on solving tomorrow's smart cities problems; from the computing and information to its facilities infrastructure. He studies road safety and road-users' behavior through the automated analysis of traffic data. He serves on the Transportation Research Board AED50 Committee on Artificial Intelligence and Advanced Computing Applications.

ADAN VELA received the Ph.D. degree in mechanical engineering from the Georgia Institute of Technology. He holds the rank of an Assistant Professor with the Industrial Engineering and Management Systems Department, University of Central Florida. Prior to his academic post, he served as a member of the Technical Staff with MIT Lincoln Laboratory. Over the past 20 years, he has developed an expertise in the modeling, simulation, and optimization of complex traffic systems, with focused research interest in those systems that involve human-in-the-loop control and intelligent decision systems.